The Journal of Immunology

Human Procaspase-1 Variants with Decreased Enzymatic Activity Are Associated with Febrile Episodes and May Contribute to Inflammation via RIP2 and NF-κB Signaling

Michael C. Heymann, Stefan Winkler, Hella Luksch, Silvana Flecks, Marcus Franke, Susanne Ruß, Seza Özen, Engin Yilmaz, Christoph Klein, Tilmann Kallinich, Dirk Lindemann, Sebastian Brenner, Gerd Ganser, Joachim Roesler, Angela Rösen-Wolff and Sigrun R. Hofmann

J Immunol 2014; 192:4379-4385; Prepublished online 4 April 2014;
doi: 10.4049/jimmunol.1203524
http://www.jimmunol.org/content/192/9/4379

The Journal of Immunology is published twice each month by
The American Association of Immunologists, Inc.,
1451 Rockville Pike, Suite 650, Rockville, MD 20852

Print ISSN: 0022-1767 Online ISSN: 1550-6606.

Human Procaspase-1 Variants with Decreased Enzymatic Activity Are Associated with Febrile Episodes and May Contribute to Inflammation via RIP2 and NF-κB Signaling

Michael C. Heymann,*[,1] Stefan Winkler,*[,1] Hella Luksch,* Silvana Flecks,* Marcus Franke,* Susanne Ruß,* Seza Özen,[†] Engin Yilmaz,[†] Christoph Klein,[‡] Tilmann Kallinich,[§] Dirk Lindemann,[¶] Sebastian Brenner,* Gerd Ganser,[‖] Joachim Roesler,* Angela Rösen-Wolff,*[,1] and Sigrun R. Hofmann*[,1]

The proinflammatory enzyme caspase-1 plays an important role in the innate immune system and is involved in a variety of inflammatory conditions. Rare naturally occurring human variants of the caspase-1 gene (*CASP1*) lead to different protein expression and structure and to decreased or absent enzymatic activity. Paradoxically, a significant number of patients with such variants suffer from febrile episodes despite decreased IL-1β production and secretion. In this study, we investigate how variant (pro) caspase-1 can possibly contribute to inflammation. In a transfection model, such variant procaspase-1 binds receptor interacting protein kinase 2 (RIP2) via Caspase activation and recruitment domain (CARD)/CARD interaction and thereby activates NF-κB, whereas wild-type procaspase-1 reduces intracellular RIP2 levels by enzymatic cleavage and release into the supernatant. We approach the protein interactions by coimmunoprecipitation and confocal microscopy and show that NF-κB activation is inhibited by anti–RIP2-short hairpin RNA and by the expression of a RIP2 CARD-only protein. In conclusion, variant procaspase-1 binds RIP2 and thereby activates NF-κB. This pathway could possibly contribute to proinflammatory signaling. *The Journal of Immunology*, 2014, 192: 4379–4385.

The proinflammatory enzyme caspase-1 plays an important role in the innate immune system and is involved in a variety of inflammatory conditions such as periodic fevers or gout. Normally, inflammasome activation results in procaspase-1 autoprocessing to generate the active form. This heterotetrameric enzyme containing two p10 and two p20 subunits is able to process the proforms of IL-1β and IL-18 into their biologically active mature forms (1–8). These cytokines subsequently participate in an appropriate response of the immune system to tissue damage or pathogen invasion (9) but also can play a role in autoinflammatory conditions (10).

Recently, we reported seven rare naturally occurring genetic variants of human procaspase-1, which exhibited altered protein structure and showed decreased or absent autoprocessing and enzymatic activity (11). However, such procaspase-1 variants with decreased activity were detected in patients with autoinflammatory disease. Thus, we discussed possible disease modifying effects of the (pro)caspase-1 variants because they may have attenuated an otherwise more severe disorder (11). In addition, Lamkanfi et al. (12) showed that procaspase-1 with a defective active center can bind receptor interacting protein kinase 2 (RIP2) and thereby activate NF-κB. This NF is known as a key player in orchestrating inflammation (13). Therefore, we explored whether the naturally occurring procaspase-1 variants also can have a proinflammatory effect.

Materials and Methods

Abs

The following Abs were used: anti–procaspase-1 A-19 (sc-622), anti–caspase-1 p20 h297 (sc-22163), and anti–RIP2 N-19 (sc-8610) all from Santa Cruz Biotechnology (Santa Cruz, CA); anti-RIP2 (PX093) from Cell Sciences (Canton, MA); anti-RIP2 (SP6266P) from Acris (Hiddenhausen, Germany); anti-RIP2 D10B11 from Cell Signaling Technology (Beverly, MA); anti-RIP2 (8427) from Abcam (Cambridge, U.K.); anti-GAPDH (H86045M) from Meridian Life Science (Saco, ME); anti-vesicular stomatitis virus (VSV) (V5507) from Sigma-Aldrich (St. Louis, MO); HRP-linked anti-rabbit (NA9340) from GE Healthcare (Freiburg, Germany); HRP linked anti-mouse (P0260) from DakoCytomation (Glostrup, Denmark); and Alexa Fluor 488–linked anti-rabbit (A-11008) and Alexa Fluor 568–linked anti-rabbit (A-11011) both from Life Technologies (Darmstadt, Germany).

Plasmids

Plasmids were encoding procaspase-1, VSV-tagged RIP2-kinase negative, and caspase activation and recruitment domain $(CARD)_{RIP2}$ and were gifts

*Klinik und Poliklinik für Kinder- und Jugendmedizin, Medizinische Fakultät der Technischen Universität Dresden, 01307 Dresden, Germany; [†]Faculty of Medicine Ankara, Hacettepe University, Sihhiye, Ankara 06100, Turkey; [‡]Department of Pediatrics, Dr. von Hauner Children's Hospital, Ludwig-Maximilians-University Munich, 80337 Munich, Germany; [§]Department for Pediatric Pneumology and Immunology, Charité Medical University of Berlin, 10117 Berlin, Germany; [¶]Institut für Virologie, Medizinische Fakultät der Technischen Universität Dresden, 01307 Dresden, Germany; and [‖]Department of Pediatric and Adolescent Rheumatology, St. Josef-Stift Sendenhorst, 48324 Sendenhorst, Germany

[1]M.C.H., S.W., A.R.-W., and S.R.H. contributed equally.

Received for publication December 24, 2012. Accepted for publication February 21, 2014.

The work was supported by the German Research Foundation (Deutsche Forschungsgemeinschaft Grants KFO249, TP1, RO/471-11, and TP2, HO 4510/1-1) and the Federal Ministry of Education and Research (PID-NET, Project A4).

Address correspondence and reprint requests to Dr. Joachim Roesler, Klinik und Poliklinik für Kinder- und Jugendmedizin, Medizinische Fakultät der Technischen Universität Dresden, Fetscherstrasse 74, 01307 Dresden, Germany. E-mail address: roeslerj@rcs.urz.tu-dresden.de

The online version of this article contains supplemental material.

Abbreviations used in this article: CARD, caspase activation and recruitment domain; cLPS, crude LPS; IRES, internal ribosome entry site; RIP2, receptor interacting protein kinase 2; shRNA, short hairpin RNA; VSV, vesicular stomatitis virus; wt, wild-type.

from Prof. J. Tschopp (University of Lausanne, Lausanne, Switzerland). The luciferase reporter plasmid pBxIVluci was a gift from Prof. G. Nuñez (University of Michigan, Ann Arbor, MI). All plasmids for procaspase-1 variants have been described in Ref. 11. RIP2-wild-type (wt) was created by site-directed mutagenesis of the VSV-tagged RIP2-kinase–negative plasmid using the QuikChange II XL Site-Directed Mutagenesis Kit from Agilent Technologies (Santa Clara, CA), according to manufacturer's protocol. The CrmA plasmid was a gift from Dr. J. Bugert (Cardiff University, Cardiff, U.K.).

Transfection protocol

For transfection, HEK 293T cells were seeded in 6-well plates, transfected 24 h later with the respective plasmids using 1.75 μg/ml polyethylenimine, and evaluated 24 h later.

NF-κB luciferase reporter assay

NF-κB activity was determined using the Luciferase Assay System from Promega (Mannheim, Germany), according to the manufacturer's protocol. The activity of the luciferase was measured sequentially on a Mithras LB940 (Berthold, Bad Wildbad, Germany).

Knockdown of RIP2 in HEK 293T cells

HEK 293T cells were transduced with anti-RIP2 short hairpin RNA (shRNA) lentiviral particles (sc-37389-V) or control shRNA lentiviral particles (sc-108080); both from Santa Cruz Biotechnology using 3 μg/ml Polybrene, according to the manufacturer's protocol. Cells were cultured in IMDM 10% FCS and selected with 4 μg/ml puromycin. Protein knockdown was analyzed by Western blotting using anti-RIP2 PX093 from Cell Sciences. Loaded protein was normalized to total protein concentration determined with DC Protein Assay from Bio-Rad (Munich, Germany).

Immunofluorescence staining

Human peripheral blood monocytes were isolated from PBMCs using CD14-magnetic beads from Miltenyi Biotec (Bergisch Gladbach, Germany) and differentiated to macrophages by incubation in M-CSF (50 ng/ml) for 7 d. The cells were then incubated with or without crude LPS (10 ng/ml) for 1 h, fixed in 4% paraformaldehyde for 10 min at 4°C, washed, and permeabilized in PBS containing 0.04% saponin and 1% BSA for 1 h. Thereafter, the cells were stained with the appropriate primary Ab for 2 h (anti-RIP2, 8427, and anti–procaspase-1 A-19), followed by staining with the secondary Ab for 45 min. Cover slips were mounted on glass slides in Vectashield mounting medium from Vector Laboratories (Burlingame, CA). Cells were imaged using a Zeiss LSM 510 confocal microscope from Carl Zeiss (Jena, Germany) or a Leica TCS SP5 from Leica Microsystems (Wetzlar, Germany) with a ×40 or a ×63 1.4NA objective lens. An argon laser was used for excitation of $Alexa^{488}$ at wavelengths of 488 nm, whereas a helium-neon laser (543 nm) was used for excitation of $Alexa^{568}$.

Quantification of colocalization has been performed with Fiji (14).

Lentiviral transduction of THP-1 cells

Expression of endogenous (pro)caspase-1 was knocked down using the shRNA expression vector plKO.1 (Addgene, Cambridge, MA). The following target sequences were used: *CASP1-3′*-untranslated region, "AAGAGATCCTTCTGTAAAGGT"; and control, "AAGACCTCTTGTTAAGAGAGT." The knockdown was confirmed by Western blotting. An internal ribosome entry site (IRES) cassette was annexed to the Flag-tagged cDNA of wt or variant C285A-procaspase-1, and the constructs were cloned into the lentiviral transfer vector pRRL.SIN.cPPT.SFFV.GFP.WPRE [provided by Prof. C. Baum, Hannover Medical School, Institute of Experimental Hematology, Hannover, Germany (15)] with the GFP downstream of the IRES. To produce lentiviral vector particles, HEK 293T cells were transfected with lentiviral transfer plasmids in combination with the plasmids psPAX2 and pVSVg. THP-1 cells were transduced with plkO.1 lentiviral stocks and selected with 1 μg/ml puromycin. Subsequently, the shRNA-expressing THP-1 cell lines were reconstituted by transduction with pRRL.SIN.cPPT.SFFV.CASP1-WT.IRES.GFP.WPRE, pRRL.SIN.cPPT.SFFV.CASP1-L265S.IRES.GFP.WPRE, or pRRL.SIN.cPPT.SFFV.GFP.WPRE stocks and sorted by FACS to enrich to >95% GFP-positive cells.

Coimmunoprecipitation using THP-1 cells

THP-1 cells were differentiated with PMA (10 ng/ml) for 24 h and stimulated with 1 μg/ml crude LPS (L5293; purchased from Sigma-Aldrich). After incubation periods as indicated, cells were lysed with lysis buffer and immunoprecipitated as described above, using anti-RIP2 N-19 for RIP2 precipitation. Densitometric analysis was performed using ImageJ (http://imagej.nih.gov/ij/).

Coimmunoprecipitation using HEK 293T cells

Cells were transfected in 6-well plates with RIP2-VSV (800 ng) and/or variants of procaspase-1-Flag (200 ng) plasmids. After 24 h, cells were lysed with lysis buffer containing 20 mM Tris/HCl (pH 7.4), 150 mM NaCl, 10 mM EDTA, 0.2% Nonidet P-40, 1 mM PMSF, and complete EDTA–free protease inhibitor (Roche Applied Science, Mannheim, Germany). Lysates were clarified and analyzed by SDS-PAGE and Western blotting using anti-VSV or anti–procaspase-1 A-19. For immunoprecipitation, lysates were incubated with anti-VSV for RIP2 precipitation or anti–procaspase-1 A-19 for 2 h at 4°C with rotation. Afterward, the immune complexes were incubated with protein G Plus–agarose from Santa Cruz Biotechnology overnight at 4°C with rotation. Precipitates were analyzed by SDS-PAGE and Western blotting. All experiments were repeated at least three times.

RIP2 cleavage experiments

For RIP2 cleavage experiments, zVAD-FMK (50 μM) from Calbiochem (catalog number 219007; Merck Millipore, Billerica, MA) was added to the cell media 3 h prior harvesting. CrmA was supplied by cotransfection of a CrmA plasmid. RIP2 protein was detected by Western blot analysis using the anti-RIP2 Ab SP6266P.

In addition, the tandem fusion construct mCherry-RIP2-EGFP was introduced into the vector p6NST51. p6NST51 is a variant of p6NST50 (16) having the SFFV U3-driven IRES EGFP-Zeo expression cassette replaced by a IRES-Zeo resistance cassette. mCherry and EGFP genes have been purchased from BD Clontech (Mountain View, CA). RIP2 protein levels were determined by Western blot using anti-RIP2 Ab PX093 (Cell Sciences) for N-terminal RIP2 and anti-RIP2 Ab D10B11 (Cell Signaling Technology) for C-terminal RIP2.

RIP2 release experiment

To study the release of RIP2, HEK 293T cells were transfected with plasmids coding for RIP2 and either wt procaspase-1 or the enzymatically inactive variant C285A. Proteins in the supernatant were precipitated with methanol/chloroforme. The cells had been cultured in media including insulin-transferrin-selenium-ethanolamine (Life Technologies) instead of FBS for the last 24 h.

Statistics

Significance of the NF-κB assay results and of Table I was determined by the paired Wilcoxon rank-test (Holm adjusted) and Fisher's exact test, respectively.

Results

Procaspase-1 variants are associated with febrile episodes

Recently, we characterized structure and function of different genetic variants of procaspase-1 (p.R221C, p.R240Q, p.N263S, p.L265S, p.T267I, p.K319R, and p.A329T) found in a healthy control population and in patients with recurrent febrile episodes (11). These procaspase-1 variants did not segregate with disease within families. Almost all relatives of patients with and without the variants were immunologically healthy. This excludes the variants from causing a monogenic disorder. However, we observed a statistically significant difference for the procaspase-1 variants to occur more often in patients than in healthy donors (Table I). Ethnicity is probably not a confounding factor because results are still significant within each group of Arabs, Turks, and whites. The rarest variants (R221C/wt, L265S/wt, T267I/wt, R240Q/R240Q, and R240Q/K319R) occur in patients only.

Taken together, these results support the assumption that at least some of the variants are disease promoting cofactors.

Procaspase-1 variants activate NF-κB

Next, we analyzed a possible mechanism that could explain how the procaspase-1 variants contributed to proinflammatory signaling. For this purpose, we transfected HEK 293T cells with plasmids coding for wt and variant procaspase-1. The artificial variant C285A with a defective active center was included as control. The release of active NF-κB from the intrinsic NF-κB/IκB complex was measured by a luciferase reporter assay. The variant R221C was only weakly expressed at the protein level (11) and therefore

Table I. Procaspase-1 variants are associated with febrile episodes within different ethnic groups

Ethnic Group	Patients[a]: Variant Alleles/ Total Alleles	Control[b]: Variant Alleles/ Total Alleles	Significance
Whites	22/800	1/214	$p = 0.03$
Turks	7/102	2/200	$p = 0.008$
Arabs	3/12	4/200	$p = 0.004$

The variant alleles comprise p.R221C, p.R240Q, p.N263S, p.L265S, p.T267I, p.K319R, and p.A329T.
[a]Patients suffer from recurrent febrile episodes.
[b]Healthy blood donors.

not analyzed in this study. The other variants (N263S, K319R, R240Q, L265S, and C285A) and wt procaspase-1 were equally expressed after transfection (Fig. 1A). Furthermore, protein levels of endogenous RIP2 were also similar (Fig. 1A). The caspase-1 variants induced an increase in NF-κB activity that was significant in R240Q, L265S, and C285A (Fig. 1B). This increase roughly correlated inversely with enzymatic activity.

Enhanced NF-κB activity was not accompanied by a increase or decrease of cell death rates of the transfected HEK 293T cells as measured by caspase-3 activation or ethidiumbromide staining of the transfected cells (Supplemental Fig. 1A, 1B). Hence, altered cell death rates do not explain differences in NF-κB activity.

The increase in NF-κB activity induced by variant procaspase-1 depends on RIP2

To investigate the participation of RIP2 in the observed enhanced NF-κB activation, we performed a cotransfection experiment with a plasmid coding for the CARD domain of RIP2 in HEK 293T cells. The coexpression of this plasmid alone abolished the procaspase-1–mediated NF-κB activation probably by blocking the

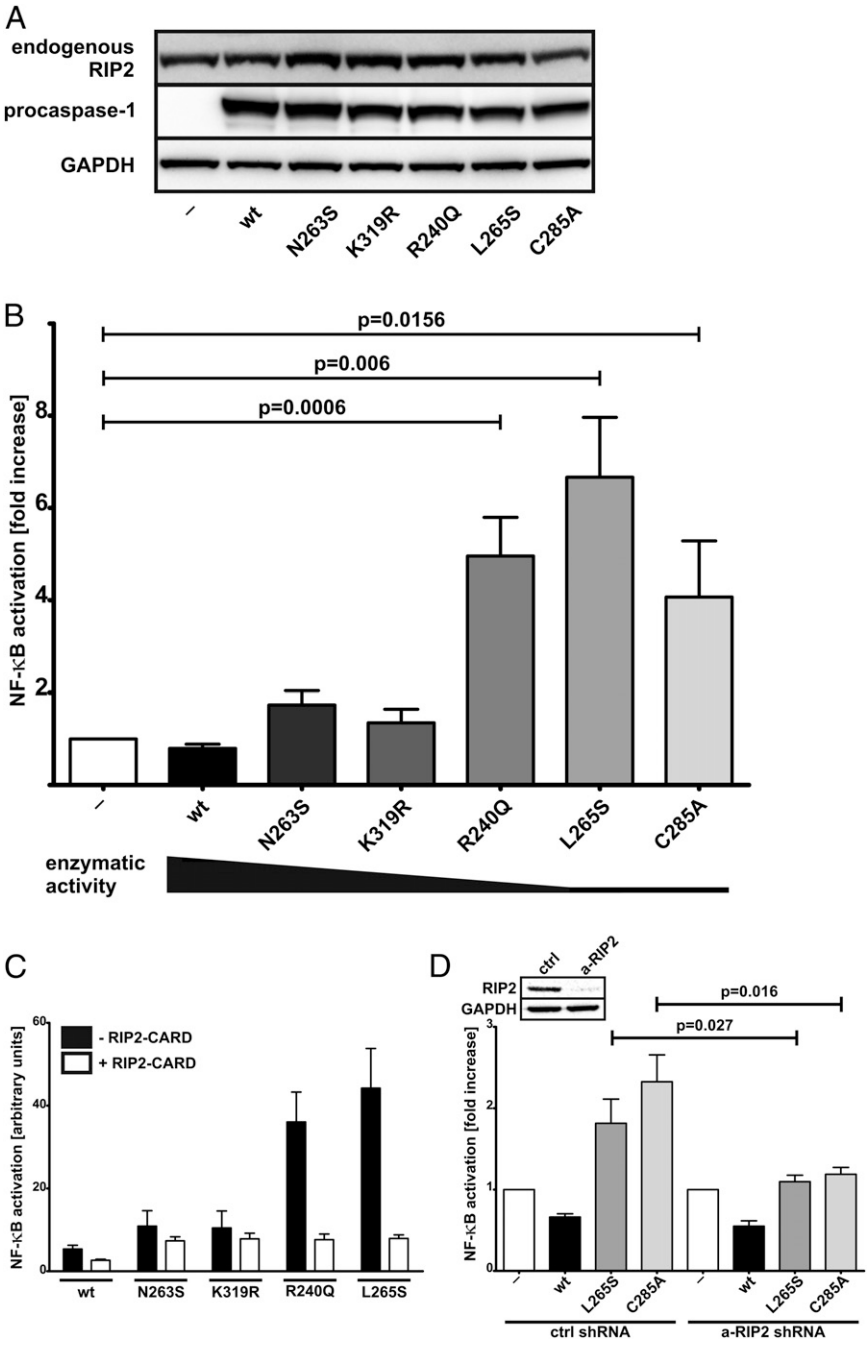

FIGURE 1. NF-κB activation by procaspase-1 variants is mediated by RIP2. (**A**) Similarity of the expression levels of endogenous RIP2 as well as the different overexpressed procaspase-1 variants in HEK 293T was illustrated by Western blot using anti-RIP2 Ab D10B11 (C-terminal; Cell Signaling Technology) and anti–caspase-1 Ab A19 (Card-Domain; Santa Cruz Biotechnology). (**B**) Fold increase of intrinsic NF-κB activation in HEK 293T cells as measured by a luciferase reporter after transfection with plasmids coding for procaspase-1 variants as compared with transfection with empty plasmid (−, set to 1), $n = 9$. (**C**) Similar to (B), but cotransfected with a plasmid coding for the CARD domain of RIP2 where indicated; ordinate: arbitrary fluorescence units of luciferase substrate, $n = 3$. (**D**) Similar to (B), but transfection with plasmids coding for procaspase-1 variants after transduction of cells with anti-RIP2 shRNA (a-RIP2) or with irrelevant control shRNA (ctrl), $n = 10$. *Inset* confirms knockdown of RIP2 by a Western blot analysis with anti-RIP2 Ab PX093 (N-terminal; Cell Sciences).

interaction of the CARD domain of procaspase-1 with the CARD domain of complete RIP2 (Fig. 1C).

Furthermore, we knocked down RIP2 in HEK 293T cells with anti–RIP2-shRNA. Strongly decreased protein levels of RIP2 were confirmed (*inset* in Fig. 1D). Knockdown of RIP2 led to a significant reduction of NF-κB activation by the variants L265S and C285A compared with control cells (Fig. 1D). Possible shRNA off-target effects were excluded using anti–RIP2-shRNA constructs targeting two additional coding sequences of RIP2 (Supplemental Fig. 2).

Taken together, these data show that the procaspase-1 variants activate NF-κB via RIP2 in a transfection model.

Interaction and colocalization of procaspase-1 and RIP2 in THP-1 cells and human macrophages

In a next step, we examined whether endogenous procaspase-1 interacts with endogenous RIP2 in cells that belong to the immune system. Therefore, native THP-1 cells, differentiated with PMA and stimulated with crude LPS (cLPS) for different time intervals, were lysed, and endogenous RIP2 was immunoprecipitated. We found that endogenous procaspase-1 coprecipitated in a time-dependent manner (Fig. 2A). The strongest RIP2–procaspase-1 interaction occurred after 60–80 min and decreased after ~3 h.

Next, we localized RIP2 and procaspase-1 in human monocyte–derived macrophages using Ab staining and confocal microscopy. After stimulation with cLPS, RIP2 and procaspase-1 colocalized in a cytoplasmic compartment adjacent to the nucleus of the macrophages. This happened in a time dependent manner and in accordance with the coimmunoprecipitation (co-IP) experiment (Fig. 2A). The highest rate of cells showing this colocalization was found 60–80 min after the beginning of cLPS stimulation (Fig. 2B, 2C). Medium exchange alone did not induce colocalization of RIP2 and procaspase-1 (Supplemental Fig. 3). The colocalization diminished over ~3 h and then reached the level of nonstimulated cells. The localization of procaspase-1 and RIP2 in the same area was further ensured by determining Pearson's correlation coefficient [which will be close to 1 if green and red channel distributions are linked (17)] and Manders' overlap coefficient (Fig. 3A). In accordance with the cell staining, fluorescence intensity profiles of both colors correlated in a corresponding histogram (Fig. 3B).

Analysis of interaction of procaspase-1 variants with RIP2 by Co-IP

To investigate the interaction of RIP2 with an inactive procaspase-1 variant, we established THP-1 cells that had been transduced with shRNA targeting a sequence of the 3′-untranslated region of wt procaspase-1 mRNA to knock down endogenous wt procaspase-1. The reconstitution with either wt procaspase-1 or the enzymatically inactive variant L265S was realized by a second transduction. Western blot analysis showed similar amounts of introduced procaspases compared with endogenous procaspase-1 in control cells (Fig. 4A, lysate, *middle row*).

Prior to IP, the cells were differentiated with PMA and stimulated with cLPS. Endogenous RIP2 levels were constant in the cell lysates (Fig. 4A, lysate, *upper row*) and in the immunoprecipitated fraction (Fig. 4A, IP: aRIP2, *upper row*). The IP of intrinsic RIP2 led to coprecipitation of reconstituted procaspase-1 (Fig. 4A, IP: a-RIP2, *bottom row*). However, interaction of the enzymatically inactive variant L265S with RIP2 was increased compared with wt procaspase-1 (Fig. 4A, IP: a-RIP2, *bottom row*). Although the enzymatically inactive variant was expressed 1.3-fold stronger than reconstituted wt procaspase-1in the lysate, the precipitation of the L265S variant with RIP2 was 2.3-fold higher as determined densitometrically.

In parallel, we cotransfected HEK 293T cells with plasmids coding for VSV-tagged RIP2 and either wt procaspase-1 or one of the enzymatically inactive variants L265S and C285A to gain higher levels of these proteins within cells. Again, IP of VSV-RIP2 led to coprecipitation of procaspase-1 and vice versa (Fig. 4B).

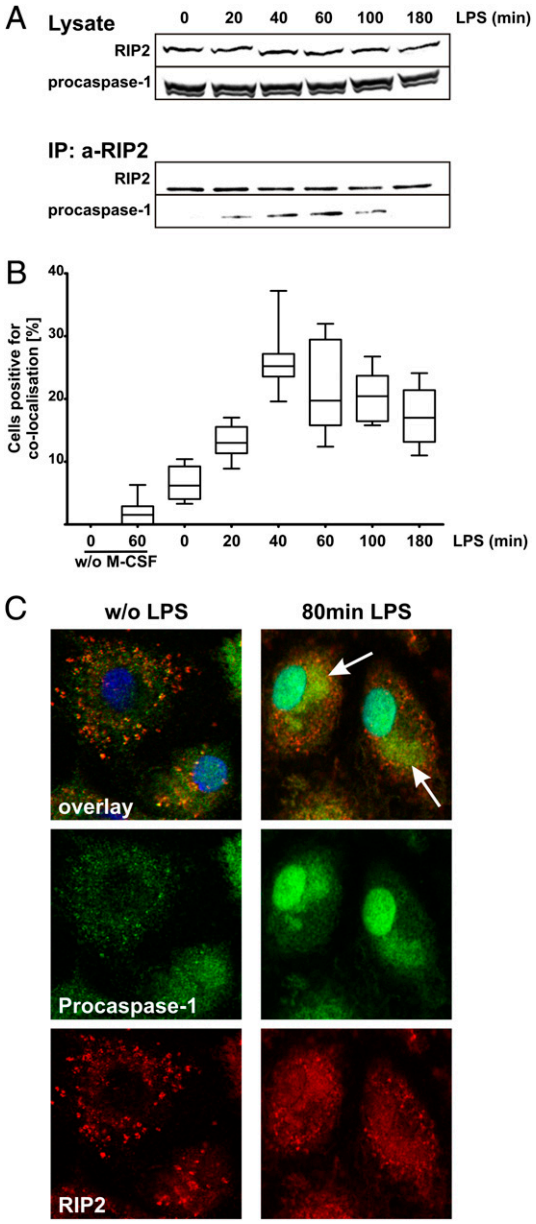

FIGURE 2. Coprecipitation and colocalization of endogenous procaspase-1 with RIP2 in human macrophages. (**A**) THP-1 cells were differentiated to macrophages with PMA (10 ng/ml, 24 h) and stimulated with LPS (1 μg/ml) for different time intervals. Lysate: constant expression of RIP2 and procaspase-1. Co-IP of endogenous procaspase-1 with endogenous RIP2 shows a time course of interaction. (**B**) Quantification of colocalization of procaspase-1 and RIP2 in monocyte-derived macrophages. A total of 1000 cells in three independent experiments has been analyzed for colocalization of procaspase-1 and RIP2. Colocalization-positive cells as shown in (**C**) have been counted after different time intervals of LPS (10 ng/ml) stimulation and are shown as percentage of total cells. Note the similarity in the time course of Co-IP in (A) and of colocalization in (B). (C) Ab staining and confocal microscopy of procaspase-1 and RIP2 in human monocyte–derived macrophages. Original magnification ×63. After stimulation with LPS, RIP2 and procaspase-1 colocalize perinuclear in the cytoplasm of the macrophages (white arrows). RIP2 is shown in the red, procaspase-1 in the green, and nuclei in the blue (DAPI) channel. *Left panel*, nonstimulated cells, *right panel*, cells after 80-min incubation with LPS. Colocalization was also seen with Abs binding to epitopes of procaspase-1 not located in the CARD domain (data not shown).

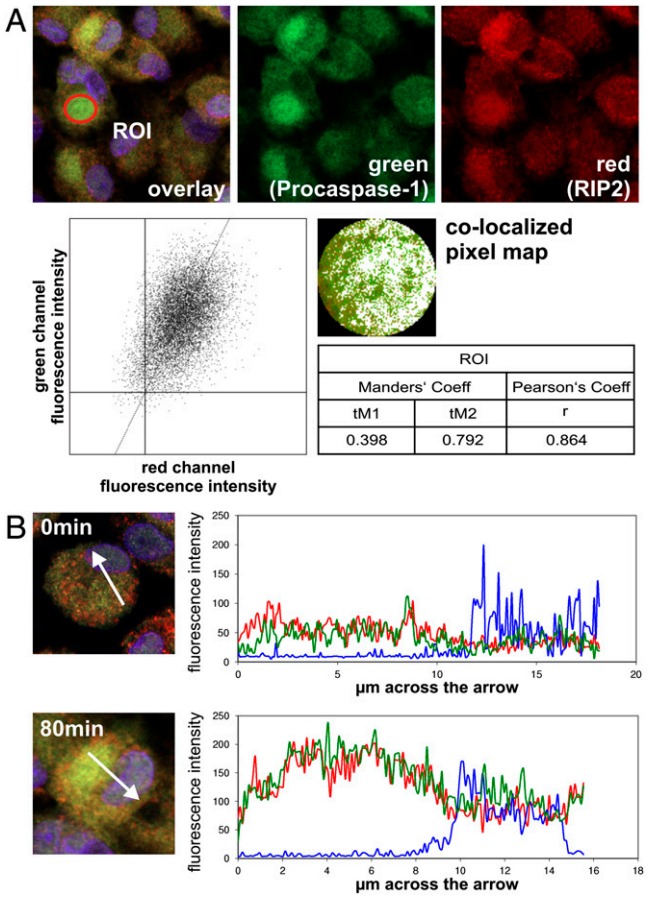

FIGURE 3. Quantitative analysis of the colocalization of procaspase-1 and RIP2 in human macrophages. (**A**) Confocal planes are shown individually or merged. For the region of interest (ROI, red circle) the Pearson's correlation coefficient and Manders' overlap coefficient are shown in the table. The scatterplot shows the correlation of green and red channels. Complete colocalization would result in a pixel distribution along a straight line whose slope will depend on the fluorescence ratio between the two channels. The spread of the pixel is quantified by the Pearson's coefficient. The colocalized pixels are shown in white in the respective map. (**B**) The histogram shows fluorescence intensity profiles across the white arrows for both green and red channels before and after stimulation with LPS. Original magnification ×63.

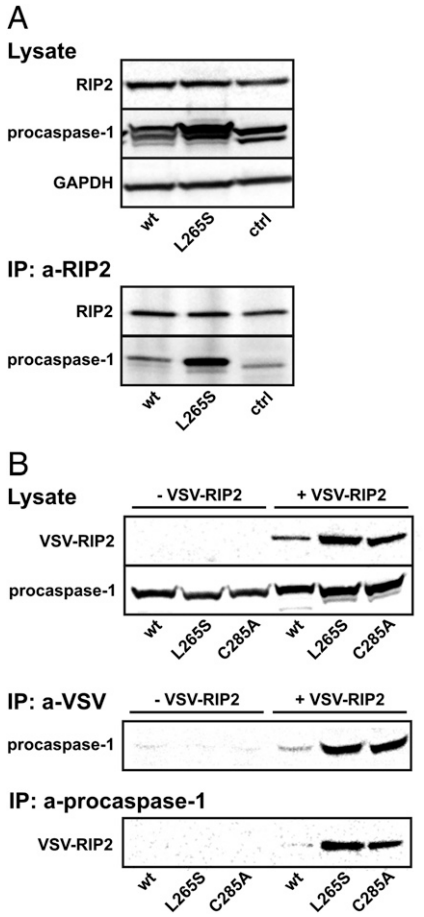

FIGURE 4. Interaction of procaspase-1 with RIP2 as demonstrated by coimmunoprecipitation. (**A**) Endogenous procaspase-1 was knocked down (by transduction) in THP-1 cells that were then reconstituted by transduction with wt or variant L265S procaspase-1. Control (ctrl) THP-1 cells were only treated with irrelevant shRNA (by transduction). The lysate shows endogenous RIP2 and transduced (wt, L265S) or endogenous procaspase-1 (ctrl), respectively. IP with an anti-RIP2 (N-19) Ab leads to coprecipitation of transduced (wt, L265S) or endogenous procaspase-1 (ctrl), respectively. The IP was performed after differentiation to macrophages (10 ng/ml PMA, 24 h) and stimulation (1 µg/ml LPS, 1 h) of the cells. (**B**) HEK 293T cells were cotransfected with plasmids coding for RIP2-VSV and procaspase-1 variants (lysate). IP with anti-VSV or anti–procaspase-1 (A19) Abs and Western blot of coprecipitating procaspase-1 or RIP2, respectively.

However, we noticed that cotransfection with a plasmid coding for wt procaspase-1 yielded much fainter VSV-RIP2 bands compared with cells cotransfected with plasmids coding for L265S or C285A variants (Fig. 4B, lysate, *upper row*). The differences of the VSV-RIP2 protein levels became even stronger in the co-IP (Fig. 4b, a-procaspase-1 IP). Similar to the anti-RIP2 IP with the transduced THP-1 cells, anti–VSV-RIP2 IP in transfected HEK 293T cells yielded much stronger bands of enzymatically inactive procaspase-1 variants compared with wt procaspase-1 (Fig. 4B, a-VSV IP).

These data indicate that interaction of enzymatically inactive procaspase-1 variants with RIP2 was enhanced.

wt but not variant procaspase-1 decreased intracellular RIP2 levels by enzymatic cleavage and by release of RIP2 into the supernatant

The previous experiments suggested decreased VSV-RIP2 protein levels in cells cotransfected with a plasmid coding for wt procaspase-1. Next, we investigated this phenomenon. First, plasmids coding for different procaspase-1 variants were transfected together with a plasmid coding for VSV-RIP2 into HEK 293T cells. In Western blot analysis, wt and enzymatically residual active procaspase-1 variants (e.g., N263S) yielded indeed fainter bands for VSV-RIP2 than inactive procaspase-1 forms (Fig. 5A). Moreover, an 8-kDa C-terminal cleavage product of RIP2 could be found when active procaspase-1 had been cotransfected (Fig. 5A).

Second, cleavage experiments with the tandem fusion protein mCherry-RIP2-EGFP (cartoon in Fig. 5B) revealed another RIP2 cleavage product at the N terminus fused to mCherry (80 kDa; Fig. 5B, *first row*). The C-terminal cleavage product fused to GFP (30 kDa) could be confirmed (Fig. 5B, *second row*).

Third, two different kinds of caspase-inhibitors, zVAD-CMK and CrmA, prevented the wt procaspase-1–mediated reduction of VSV-RIP2 protein level in the lysate (Fig. 5C).

Finally, we tested the hypothesis that coexpression of wt procaspase-1 with VSV-RIP2 induces the release of VSV-RIP2 into the supernatant. As shown in Fig. 5D, VSV-RIP2 could be detected in the supernatant of cells, which had been cotransfected with a plasmid coding for wt procaspase-1 in contrast to cells with the inactive variant C285A or without procaspase-1 (Fig. 5D, supernatant). This release of VSV-RIP2 correlated with a reduction of intracellular VSV-RIP2 protein level (Fig. 5D, lysate). Activation

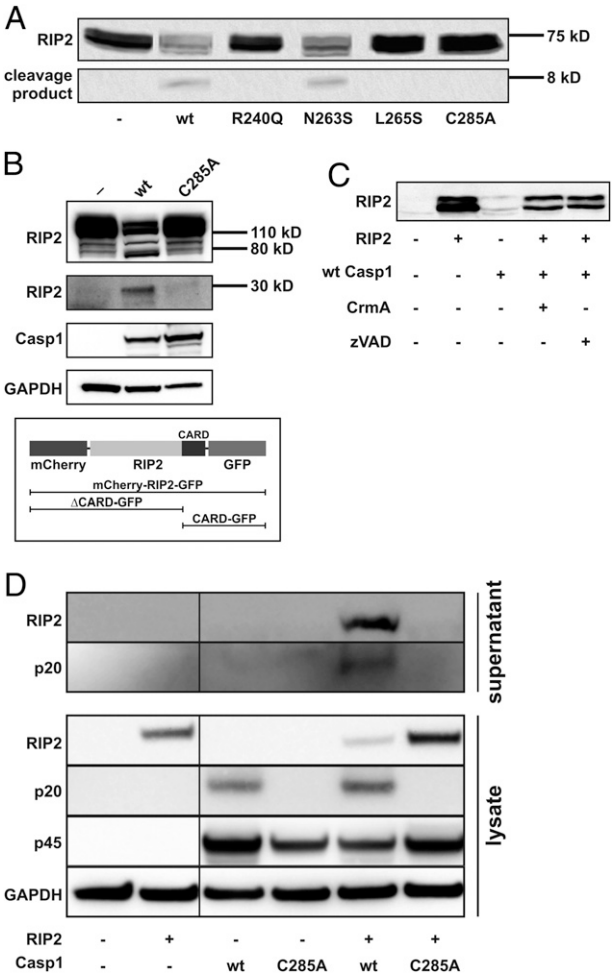

FIGURE 5. RIP2 gets cleaved and released from the cells dependent on the enzymatic activity of caspase-1. (**A**) Western blot with anti-RIP2 Ab (SP6266P, C-terminal) after cotransfection of HEK 293T cells with plasmids coding for wt RIP2 and procaspase-1 variants shows a RIP2 cleavage product depending on enzymatically active caspase-1. (**B**) Confirmation of N-terminal (N-t.) cleavage product of RIP2. The tandem protein mCherry-RIP2-EGFP is cut by wt procaspase-1 yielding a C-terminal (C-t.) cleavage product of ~30 kDa from RIP2 that is fused to GFP (the band in the *second row* also can be stained with an anti-GFP Ab, data not shown, in this study stained with anti-RIP2 Ab D10B11, C-terminal). The multiple bands in the *first row* are generated by cutting RIP2 and also the annexed dyes (anti-RIP2 Ab PX093, N-terminal). (**C**) Similar Western blot as in A after cotransfection with plasmids coding for wt RIP2 and wt procaspase-1, and addition of the caspase inhibitors zVAD or CrmA (by cotransfection). (**D**) Western blot of lysate and precipitated supernatant of HEK 293T cells transfected with plasmids coding for VSV-RIP2 and procaspase-1 wt or the enzymatically inactive variant C285A. The protein levels had been determined using the following Abs: anti-RIP2 Ab PX093 (N-terminal; Cell Sciences), anti–caspase-1 cleaved p20 Ab h297 (Santa Cruz Biotechnology) for cleaved caspase-1 subunit p20 (p20), anti-GAPDH Ab H86045M (Meridian Life Science), and anti–caspase-1 Ab A19 (Santa Cruz Biotechnology) for procaspase-1 p45 (p45).

of wt caspase-1 was confirmed by the detection of p20 in the lysate, independent of VSV-RIP2 cotransfection. The p20 subunit was not detected in cells expressing the inactive variant C285A (Fig. 5D, lysate). However, p20 was only released into the supernatant of cells, which had been cotransfected with a plasmid coding for VSV-RIP2 and wt procaspase-1 (Fig. 5D, supernatant).

These data indicate that wt procaspase-1 but not enzymatically inactive procaspase-1 variants contributed to the reduction of intracellular VSV-RIP2 levels by enzymatic cleavage and by its release into the supernatant of transfected HEK 293T cells.

Discussion

Recently, we have described human hypomorphic genetic variants of procaspase-1 (11). Phagocytes and especially monocytes from individuals with such variants show a trend to produce decreased amounts of active IL-1β (11). Therefore, such individuals should be less prone to develop autoinflammation than others. Unexpectedly, we find a significant correlation between enzymatic less or inactive procaspase-1 variants and the development of autoinflammatory disorders (Table I). In an attempt to solve this paradox, we refer to the suggestion of Lamkanfi et al. (12) and investigate the ability of the naturally occurring human procaspase-1 variants to activate NF-κB via RIP2 interaction.

In a transfection model with endogenous RIP2, we find indeed a robust activation of intrinsic NF-κB by naturally occurring hypomorphic procaspase-1 variants (Fig. 1B). Interestingly, this activation is roughly inversely proportional to the residual enzymatic activity of the variants. It depends on RIP2 and is mediated by CARD/CARD interaction between procaspase-1 and RIP2 (Fig. 1C, 1D). In accordance with this interaction, endogenous RIP2 and procaspase-1 coimmunoprecipitate (Fig. 2A). Moreover, the endogenous proteins colocalize after activation of monocyte-derived macrophages (Figs. 2C, 3) and therefore putatively interact and take part in the same molecular pathways. Using transduction of THP-1 cells with procaspase-1 variants by lentiviral vectors with limited copy numbers per cell, we avoid strong protein overexpression and approximate a physiologic situation (Fig. 4A). As indicated by coimmunoprecipitation, interaction of the enzymatically inactive procaspase-1 variant L265S with endogenous RIP2 is stronger than the respective interaction with wt procaspase-1. Co-IP of procaspase-1 and VSV-RIP2 coexpressed in transfected HEK 293T cells strongly supports the data obtained in THP-1 cells. Enzymatically inactive procaspase-1 variants interact much stronger with RIP2 than wt procaspase-1 (Fig. 4B).

The activation of NF-κB by enzymatic inactive procaspase-1 described in our study is in accordance with the data from Lamkanfi et al. (12). However, in contrast to their study, we avoid wt procaspase-1–mediated cell death (Supplemental Fig. 1A) by reducing caspase-1 expression levels. Moreover, we show equal protein

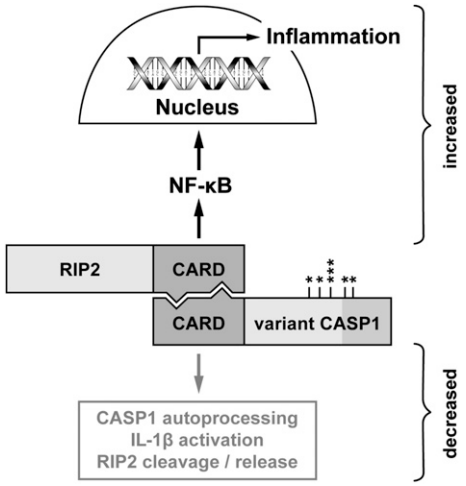

FIGURE 6. Model for proinflammatory effects induced by procaspase-1 variants with reduced enzymatic activity. The procaspase-1 variants exhibit reduced or absent enzymatic activity because of the different missense mutations, which are substituted by asterisks (from the left to the right: p.R221C, p.R240Q, p.N263S, p.L265S, p.T267I, p.K319R, and p.A329T). Although procaspase-1 autoprocessing and IL-1β activation is decreased by such procaspase-1 variants (*bottom*), the NF-κB activation is increased (*top*) as a result of the longer and/or stronger interaction between procaspase-1 and RIP2. The enhanced NF-κB activity may contribute to the transcription of proinflammatory proteins and thereby aggravate or unmask inflammatory disorders.

levels of wt procaspase-1 and all variants analyzed for NF-κB activation (Fig. 1A). Thereby, we are able to compare the NF-κB activating potential of different procaspase-1 variants with wt procaspase-1. We show an increased NF-κB activation mediated by variant procaspase-1. The underlying mechanism may be similar to NF-κB activation after binding of RIP2 to nucleotide-binding oligomerization domain-containing protein 2 (18). Hypothetically, the procaspase-1 variants with residual or no enzymatic activity induce longer NF-κB activation compared with wt procaspase-1 mediated by a longer and/or stronger interaction with RIP2. NF-κB can subsequently bind to regulatory sequences of genes that encode proinflammatory proteins and thereby upregulate their expression (13).

In contrast to enzymatically inactive procaspase-1, wt procaspase-1, and procaspase-1 variants with residual activity (e.g., N263S) reduce intracellular levels of overexpressed RIP2 (Fig. 5A). This effect as well as the faint VSV-RIP2 bands in the immunoprecipitation experiments (Fig. 4B) can be explained by RIP2 cleavage and release from cells induced by wt procaspase-1 (Fig. 5). The activation of caspase-1 and the simultaneous release of the p20 subunit by cotransfection of plasmids coding for wt procaspase-1 with RIP2 indeed has already been described (19). In this study, we additionally show the release of the overexpressed RIP2 from the cells. To our knowledge, cleavage of RIP2 by endogenous proteases has not been published to date.

So far, reduced enzymatic activity of caspase-1 realized by inhibition or knockout in mice is mainly thought to decrease inflammation (20–23). Considering the data of Kayagaki et al. (24), most studies on *Casp1* knockout mice have been performed with a *Casp1/Casp11* double knockout strain. Therefore, the described reduction of inflammatory effects cannot be linked to *Casp1* deletion with certainty. Furthermore, Osuka et al. (25) published data indicating a proinflammatory cytokine response and increased mortality in burn-injured mice treated with AC-YVAD-CMK. In addition, Menzel et al. (26) described a proinflammatory cytokine response and increased organ damage for *Casp1* knockout mice in a model for hemorrhagic shock. These data may support our hypothesis as well as the model postulated by Lamkanfi et al. (12) in vivo.

Our patients are either heterozygous or exhibit at least residual enzymatic (pro)caspase-1 activity (11). If the transfection model really applies to these patients, the remaining enzymatic activity could diminish the proinflammatory effect of the less active or inactive procaspase-1 variants by limiting protein interactions and hence limiting NF-κB activation. This may explain an only moderate in vivo effect of variant procaspase-1 that cannot be easily detected in patients' cells [e.g., by enhanced levels of IL-6, IL-8 and TNF-α secreted by monocytes from the patients (11)]. However, considering our results discussed so far, it remains unsettled if the transfection model yields mere artifacts because of protein overexpression or if the model may really apply to the in vivo situation.

Taken together, our study supports the following hypothesis (Fig. 6): Our patients are prone to autoinflammation. The procaspase-1 variants are disease modifying factors. As depicted in Fig. 6, they may promote inflammatory diseases by increased binding of RIP2 via CARD/CARD interaction and thereby induce an enhanced proinflammatory NF-κB signal. This signal may aggravate a manifest autoinflammatory disorder. It also may increase inflammation in predisposed patients above a certain threshold and thereby unmask such a disease.

Acknowledgments

We thank Prof. Jürg Tschopp (University of Lausanne) for pasmids for procaspase-1, VSV-tagged RIP2-kinase negative, CARDRIP2, and pro–IL-1β and Prof. Gabriel Nuñez (University of Michigan) for the luciferase reporter plasmid pBxIVluci. We also thank Diana Paul and Kathrin Höhne for excellent technical assistance.

Disclosures

The authors have no financial conflicts of interest.

References

1. Thornberry, N. A., H. G. Bull, J. R. Calaycay, K. T. Chapman, A. D. Howard, M. J. Kostura, D. K. Miller, S. M. Molineaux, J. R. Weidner, J. Aunins, et al. 1992. A novel heterodimeric cysteine protease is required for interleukin-1β processing in monocytes. *Nature* 356: 768–774.
2. Gu, Y., K. Kuida, H. Tsutsui, G. Ku, K. Hsiao, M. A. Fleming, N. Hayashi, K. Higashino, H. Okamura, K. Nakanishi, et al. 1997. Activation of interferon-γ inducing factor mediated by interleukin-1β converting enzyme. *Science* 275: 206–209.
3. Schmitz, J., A. Owyang, E. Oldham, Y. Song, E. Murphy, T. K. McClanahan, G. Zurawski, M. Moshrefi, J. Qin, X. Li, et al. 2005. IL-33, an interleukin-1-like cytokine that signals via the IL-1 receptor-related protein ST2 and induces T helper type 2-associated cytokines. *Immunity* 23: 479–490.
4. Cayrol, C., and J. P. Girard. 2009. The IL-1-like cytokine IL-33 is inactivated after maturation by caspase-1. *Proc. Natl. Acad. Sci. USA* 106: 9021–9026.
5. Dinarello, C. A. 2009. Immunological and inflammatory functions of the interleukin-1 family. *Annu. Rev. Immunol.* 27: 519–550.
6. Heymann, M. C., and S. R. Hofmann. 2011. Novel inflammasomes and type II diabetes, intestinal inflammation and psoriasis as newly inflammasome-related diseases. *J. Genet. Syndr. Gene Ther.* S3: 001.
7. Hofmann, S. R., M. C. Heymann, A. Hermsdorf, and A. Roesen-Wolff. 2011. Recent advances in autoinflammatory diseases and animal models. *J. Genet. Syndr. Gene Ther.* S3: 002.
8. Ghayur, T., S. Banerjee, M. Hugunin, D. Butler, L. Herzog, A. Carter, L. Quintal, L. Sekut, R. Talanian, M. Paskind, et al. 1997. Caspase-1 processes IFN-γ-inducing factor and regulates LPS-induced IFN-γ production. *Nature* 386: 619–623.
9. Shaw, P. J., M. F. McDermott, and T. D. Kanneganti. 2011. Inflammasomes and autoimmunity. *Trends Mol. Med.* 17: 57–64.
10. Heymann, M. C., and A. Rösen-Wolff. 2013. Contribution of the inflammasomes to autoinflammatory diseases and recent mouse models as research tools. *Clin. Immunol.* 147: 175–184.
11. Luksch, H., M. J. Romanowski, O. Chara, V. Tüngler, E. R. Caffarena, M. C. Heymann, P. Lohse, I. Aksentijevich, E. F. Remmers, S. Flecks, et al. 2013. Naturally occurring genetic variants of human caspase-1 differ considerably in structure and the ability to activate interleukin-1β. *Hum. Mutat.* 34: 122–131.
12. Lamkanfi, M., M. Kalai, X. Saelens, W. Declercq, and P. Vandenabeele. 2004. Caspase-1 activates nuclear factor of the κ-enhancer in B cells independently of its enzymatic activity. *J. Biol. Chem.* 279: 24785–24793.
13. Hoffmann, A., and D. Baltimore. 2006. Circuitry of nuclear factor κB signaling. *Immunol. Rev.* 210: 171–186.
14. Schindelin, J., I. Arganda-Carreras, E. Frise, V. Kaynig, M. Longair, T. Pietzsch, S. Preibisch, C. Rueden, S. Saalfeld, B. Schmid, et al. 2012. Fiji: an open-source platform for biological-image analysis. *Nat. Methods* 9: 676–682.
15. Schambach, A., M. Galla, U. Modlich, E. Will, S. Chandra, L. Reeves, M. Colbert, D. A. Williams, C. von Kalle, and C. Baum. 2006. Lentiviral vectors pseudotyped with murine ecotropic envelope: increased biosafety and convenience in preclinical research. *Exp. Hematol.* 34: 588–592.
16. Amer, D. A., G. Kretzschmar, N. Müller, N. Stanke, D. Lindemann, and G. Vollmer. 2010. Activation of transgenic estrogen receptor-β by selected phytoestrogens in a stably transduced rat serotonergic cell line. *J. Steroid Biochem. Mol. Biol.* 120: 208–217.
17. Bolte, S., and F. P. Cordelières. 2006. A guided tour into subcellular colocalization analysis in light microscopy. *J. Microsc.* 224: 213–232.
18. Ogura, Y., N. Inohara, A. Benito, F. F. Chen, S. Yamaoka, and G. Nunez. 2001. Nod2, a Nod1/Apaf-1 family member that is restricted to monocytes and activates NF-κB. *J. Biol. Chem.* 276: 4812–4818.
19. Humke, E. W., S. K. Shriver, M. A. Starovasnik, W. J. Fairbrother, and V. M. Dixit. 2000. ICEBERG: a novel inhibitor of interleukin-1β generation. *Cell* 103: 99–111.
20. Kuida, K., J. A. Lippke, G. Ku, M. W. Harding, D. J. Livingston, M. S. Su, and R. A. Flavell. 1995. Altered cytokine export and apoptosis in mice deficient in interleukin-1β converting enzyme. *Science* 267: 2000–2003.
21. Li, P., H. Allen, S. Banerjee, S. Franklin, L. Herzog, C. Johnston, J. McDowell, M. Paskind, L. Rodman, J. Salfeld, et al. 1995. Mice deficient in IL-1β-converting enzyme are defective in production of mature IL-1β and resistant to endotoxic shock. *Cell* 80: 401–411.
22. Maslanik, T., L. Mahaffey, K. Tannura, L. Beninson, B. N. Greenwood, and M. Fleshner. 2013. The inflammasome and danger associated molecular patterns (DAMPs) are implicated in cytokine and chemokine responses following stressor exposure. *Brain Behav. Immun.* 28: 54–62.
23. Liang, D. Y., X. Li, W. W. Li, D. Fiorino, Y. Qiao, P. Sahbaie, D. C. Yeomans, and J. D. Clark. 2010. Caspase-1 modulates incisional sensitization and inflammation. *Anesthesiology* 113: 945–956.
24. Kayagaki, N., S. Warming, M. Lamkanfi, L. Vande Walle, S. Louie, J. Dong, K. Newton, Y. Qu, J. Liu, S. Heldens, et al. 2011. Non-canonical inflammasome activation targets caspase-11. *Nature* 479: 117–121.
25. Osuka, A., M. Hanschen, V. Stoecklein, and J. A. Lederer. 2012. A protective role for inflammasome activation following injury. *Shock* 37: 47–55.
26. Menzel, C. L., Q. Sun, P. A. Loughran, H. C. Pape, T. R. Billiar, and M. J. Scott. 2011. Caspase-1 is hepatoprotective during trauma and hemorrhagic shock by reducing liver injury and inflammation. *Mol. Med.* 17: 1031–1038.